

# A first-principles electronic structure study of the high-symmetry surfaces of fcc americium

D. Gao, A.K. Ray\*

*Department of Physics, University of Texas at Arlington, Arlington, TX 76019, United States*

Received 20 June 2006; received in revised form 28 September 2006; accepted 4 October 2006

Available online 20 November 2006

## Abstract

Full-potential all-electron density-functional calculations with mixed basis APW + lo/LAPW have been carried out to investigate the electronic and geometric properties of the (1 1 0) surface of fcc Am(II) and compared with the corresponding properties of the (1 1 1) and (0 0 1) surfaces. In particular, the quantum size effects in the surface energies and the work functions of the (1 1 0) ultra-thin films up to seven layers at the anti-ferromagnetic ground state with spin-orbit coupling (AFM-SO) have been studied and compared with those of the (1 1 1) and (0 0 1) surfaces. A strong quantum size effect of work function up to seven layers in the fcc Am (1 1 0) surfaces is observed. The work function of the (1 1 0) surface is predicted to be 2.86 eV to be compared with 2.93 and 3.06 eV for (0 0 1) and (1 1 1) films at the ground state, respectively. On the other hand, the surface energy becomes relatively stable once the number of layers reaches three for all three surfaces. Density of states show that the 5f electrons in all three fcc Am surfaces are primarily localized. In addition, the present work of fcc Am high symmetry surfaces has been compared in detail with the corresponding available  $\delta$ -Pu surface studies.

© 2006 Elsevier B.V. All rights reserved.

PACS: 71.15.-m; 71.27+a; 73.20.At; 75.50.Ee

Keywords: Actinides; Americium; Density functional theory; Localizations; 5f electrons

## 1. Introduction

Considerable theoretical efforts have been devoted to studying the electronic and geometric structures and related properties of surfaces to high accuracy in recent years. Actinides, as a group of strongly correlated and heavy fermion systems, especially have received notable increasing interests [1–5]. As is known, experimental work on actinides is relatively difficult to perform due to material problems and toxicity. On the other hand, they play important roles in advanced nuclear fuel cycles. Hence, theoretical studies are crucial for these high-Z elements. Such studies may also lead to a better understanding of the detailed surface corrosion mechanisms in the presence of environmental gases and thus help to address the environmental consequences of nuclear materials.

Among the actinides, the unique electronic properties of americium (Am), which was first successfully synthesized and isolated at the wartime Metallurgical Laboratory [6],

have received increased interests recently, from both scientific and technological points of view. It has been noted that Am occupies a pivotal position in the actinide series with regard to the behavior of 5f electrons [7]. Atomic volumes of the actinides as a function of atomic number have experimentally displayed a sharp increase between Pu and Am [8]. In contrast to this sharp increase, the atomic volumes of the actinides before Pu continuously decreases as a function of increasing atomic number from Ac until Np, which is analogous to d transition metals. These behaviors reveal that the properties of the 5f electrons change dramatically starting from somewhere between Pu and Am. It has been suggested [9,10] that the 5f electrons of the actinides before Am participate in bonding while the 5f electrons of the actinides after Pu become localized and non-bonding. Both theoretical calculations [11] and the X-ray and high-resolution UV photoemission study [12] of the 5f electrons in Am have supported the localized picture for Am. Another notable feature is the high-pressure behavior of americium. As pressure increases, the crystal structures of americium display the following phase transitions [13]: double hexagonal close packed (Am I)  $\rightarrow$  face-centered cubic

\* Corresponding author. Tel.: +1 817 272 2503; fax: +1 817 272 3637.

E-mail address: akr@uta.edu (A.K. Ray).

(Am II)  $\rightarrow$  face-centered orthorhombic (Am III)  $\rightarrow$  primitive orthorhombic (Am IV). Although experimental data indicates that the phase transition from Am II to Am III is probably accompanied with the 5f electron delocalization [7,13], recent density functional studies by Pénicaud [14] regarding the high-pressure behavior of americium found that only the fourth phase (Am IV) is delocalized and the 5f electrons of the three previous americium phases are localized. The dynamical mean field theory calculations by Savrasov et al. [15] also indicate that the location of the Mott transition is near the Am III to Am IV boundary and that the f electrons start to participate in bonding in the highly pressurized Am IV structure. On the other hand, density functional calculations using the full-potential linear muffin-tin orbital (FP-LMTO) method by Söderlind and Landa [16] indicate that the Am I phase is stabilized by contributions from the d shell to the cohesion whereas all other phases follow from 5f electron bonding, *i.e.*, delocalization. Such controversies clearly indicate that further experimental and theoretical studies are needed to improve our understanding of americium and the associated 5f electrons.

Another controversy surrounding Am is the question of magnetism. Experimental results, in general, indicate that Am is non-magnetic. For example, Naegele et al. [12], in their photoemission study of the localization of 5f electrons in Am, assumed the ground-state electron configuration to be  $5f^6$  (non-magnetic). Huray et al. [17] in their experimental studies of the magnetism of the heavy 5f elements also found Am to have zero effective magnetic moment with an  $f^6$  probable ion configuration. Both Gouder et al. and Cox et al. [18], in their respective photoemission studies, found Am to have localized f states in a  $5f^6$  configuration, consistent with the absence of magnetic order. On the other hand, theoretical studies on Am metal, mostly based on *ab initio* self-consistent density functional theory, in general, indicate the presence of magnetism [16,19–21]. Using fully relativistic, full-potential linear-muffin-tin-orbital calculations, Eriksson and Wills [20] reported strong disagreements with experimental data. Using the same method as also canonical band theory, Söderlind and Landa [16] actually found the fcc phase to be stable by a small margin over dhcp but when d contribution is included, their energies were degenerate. They also found that the 5f electrons in Am almost entirely spin-polarize. Pénicaud [14] modeled the localization of the 5f electrons by an anti-ferromagnetic (AFM) configuration found to have a lower energy than a ferromagnetic configuration. Using the full potential Dirac relativistic basis, spin-polarized linearized-augmented-plane-wave method, Kutepov and Kutepova [21] found also the AFM ordering to be favored for dhcp Am. The around-men-field LSDA + U (AMF-LSDA + U) correlated band theory has been applied by Shick et al. [22] to study the electronic and magnetic structure of fcc-Pu-Am alloys. For fcc Am, they performed AMF-LSDA + U calculations, varying the Coulomb U from 3 to 4 eV and keeping the inter-atomic exchange parameter J at 0.75 eV. The calculations yielded practically zero magnetic moment, with an equilibrium atomic volume of  $186 \text{ (a.u.)}^3$  and a bulk modulus of 55.1 GPa with  $U=4 \text{ eV}$ . Kotliar and Vollhardt [23] have used dynamical-mean-field-theory (DMFT) approach to study strongly correlated systems,

such as the actinides. Using a DMFT-based spectral density functional approach, they observed that the f electrons in Am at zero pressure exists in a  $f^6 7F_0$  configuration, with a U value of about 4.5 eV. Our calculations [19], using the FP-LAPW method, yielded an AFM state, with an equilibrium atomic volume of  $195.3 \text{ (a.u.)}^3$  and a bulk modulus of 28.1 GPa. The experimental equilibrium volume is  $198.5 \text{ (a.u.)}^3$  and a bulk modulus of 29.4 GPa. On the other hand, results at the NSP-SO level produce an equilibrium atomic volume of  $137.8 \text{ (a.u.)}^3$  and a bulk modulus of 63.8 GPa. Thus, a non-magnetic calculation produces an error of 31% in the atomic volume and 117% in the bulk modulus! Savrasov et al. [15] have found that a non-magnetic GGA calculation failed catastrophically in reproducing the equilibrium volume of the soft phase of Am by about 50%. Clearly, there is strong disagreement here between theory and experiment as far as the question of magnetism is concerned. Given this wide spectrum of results on Am, we believe that a systematic and fully relativistic density functional study of Pu and Am surface chemistry and physics using the same level of theory could certainly lead to significant insights and knowledge about the actinides and at the very least, produce a qualitative trend in our understanding of the light to heavy actinides and stimulate further work in actinides.

The electronic structure of americium, wherein six f electrons presumably form an inert core, decoupled from the spd electrons that control the physical properties of the material, also contributes to the superconductivity in Am [24,25]. Recently, a study of the superconductivity in americium [26] as a function of pressure has showed that such studies may be an effective method to understand the unique 5f electron properties of americium including the Mott transition, *i.e.*, the evolution of the 5f electrons from localized to the delocalized.

Another effective way to probe the actinides (including americium) 5f electron properties and their roles in chemical bonding is the study of their surface properties. The unusual aspects of the bonding in bulk Am are apt to be enhanced at a surface or in a thin layer of Am adsorbed on a substrate, as a result of the reduced atomic coordination of a surface atom and the narrow bandwidth of surface states. Thus, Am surfaces and thin films may also provide valuable information about the bonding in Am. We have recently reported the bulk and surface properties of fcc  $\delta$ -Pu and atomic and molecular adsorptions on such surfaces and also bulk and (1 1 1) and (0 0 1) surfaces of fcc Am II [19,27]. As a continuation of our systematic and fully relativistic density functional studies of actinide surface physics and chemistry, in this work, we report, in some detail the electronic structure properties of fcc Am (1 1 0) surface and compare them with the corresponding properties of the other two surfaces. Other motivations for such a study also stem from the following observations: (1) both plutonium and americium represent the boundary between the “light” actinides, Th to Pu, and the “heavy” actinides, Am and beyond; (2) whereas, Pu has an open shell of f electrons, Am is closer to a full  $j = 5/2$  shell; (3) the transition from delocalization-to-localization supposedly takes place somewhere between Pu and Am; yet there is no such apparent transition observed, at least, in  $\alpha$ -Pu although the 5f electrons of  $\delta$ -Pu are partially localized [1–10,15,23,27], as

indicated by its atomic volume, which is approximately halfway between  $\alpha$ -Pu and Am.

The present study has thus focused on the (1 1 0) surfaces of Am II, which has the same fcc crystal structure as that of  $\delta$ -Pu. For such studies, it is common practice to model the surface of a semi-infinite solid with an ultra thin film (UTF), which is thin enough to be treated with high-precision density functional calculations, but is thick enough to realistically model the semi-infinite surface. Determination of an appropriate UTF thickness is complicated by the existence of possible quantum oscillations in UTF properties as a function of thickness, the so-called quantum size effect (QSE). These oscillations were first predicted by calculations on jellium films [28,29] and were subsequently confirmed by band-structure calculations on free-standing UTFs composed of discrete atoms [30–33]. The adequacy of the UTF approximation obviously depends on the size of any QSE in the relevant properties of the model film. Thus, it is important to determine the magnitude of the QSE in a given UTF prior to using that UTF as a model for the surface. This is particularly important for Am films, since the strength of the QSE is expected to increase with the number of valence electrons [28].

## 2. Computational method

The computations reported in this work have been carried out using the full-potential all-electron method with mixed basis APW + lo/LAPW method implemented in the WIEN2k software [34,35]. The generalized-gradient-approximation (GGA) to density functional theory [36] with a gradient corrected Perdew–Berke–Ernzerhof (PBE) exchange-correlation functional [37] is used and the Brillouin-zone integrations are conducted by an improved tetrahedron method of Blöchl–Jepsen–Andersen [38]. In the WIEN2k code, the alternative basis set APW + lo is used inside the atomic spheres for the chemically important orbitals that are difficult to converge, whereas LAPW is used for others. The local orbitals scheme leads to significantly smaller basis sets and the corresponding reductions in computing time, given that the overall scaling of LAPW and APW + lo is given by  $N^3$ , where  $N$  is the number of atoms. Also, results obtained with the APW + lo basis set converge much faster and often more systematically towards the final value [39]. As far as relativistic effects are concerned, core states are treated fully relativistically in WIEN2k and for valence states, two levels of treatments are implemented: (1) a scalar relativistic scheme that describes the main contraction or expansion of various orbitals due to the mass-velocity correction and the Darwin s-shift [40] and (2) a fully relativistic scheme with spin-orbit coupling included in a second variational treatment using the scalar-relativistic eigen functions as basis [41,42]. The present computations have been carried out at both scalar-relativistic and fully relativistic levels to determine the effects of relativity. To calculate the total energy, a constant muffin-tin radius ( $R_{\text{mt}}$ ) of 2.60 a.u. is used and the plane-wave cut-off  $K_{\text{cut}}$  is determined by  $R_{\text{mt}}K_{\text{cut}} = 9.0$  for all calculations. The surfaces of Am II are modeled by periodically repeated slabs of  $N$  Am layers (with one atom per layer and  $N = 1-7$ ) separated by an 80 a.u. vacuum gap. Twenty-one irreducible  $K$  points have been used for

Table 1

Surface energies  $E_s$  and work functions  $W$  for fcc Am (1 1 0), (0 0 1) and (1 1 1) films with  $N$  layers ( $N = 1-7$ ) at AFM-SO level

$N$	Surface	$W$ (eV)	$E_s$ (J/m <sup>2</sup> )
1	(1 1 0)	2.75	0.88
	(0 0 1)	2.86	0.93
	(1 1 1)	3.02	0.89
2	(1 1 0)	2.90	1.08
	(0 0 1)	2.90	0.85
	(1 1 1)	3.09	0.82
3	(1 1 0)	2.91	1.04
	(0 0 1)	2.91	0.82
	(1 1 1)	2.96	0.81
4	(1 1 0)	2.94	1.04
	(0 0 1)	2.96	0.81
	(1 1 1)	3.08	0.80
5	(1 1 0)	2.82	1.03
	(0 0 1)	2.89	0.81
	(1 1 1)	3.05	0.81
6	(1 1 0)	2.84	1.03
	(0 0 1)	2.96	0.82
	(1 1 1)	3.04	0.81
7	(1 1 0)	2.86	1.04
	(0 0 1)	2.93	0.82
	(1 1 1)	3.06	0.81

reciprocal-space integrations. For each calculation, the energy convergence criterion is set to be 0.01 mRy. Six theoretical levels of approximation, namely NSP-NSO (non-spin-polarized-no-spin-orbit coupling), NSP-SO (non-spin-polarized-spin-orbit coupling), SP-NSO (spin-polarized-no-spin-orbit coupling), SP-SO (spin-polarized-spin-orbit-coupling), AFM-NSO (anti-ferromagnetic-no-spin-orbit-coupling), and AFM-SO (anti-ferromagnetic-spin-orbit-coupling) have been implemented in our calculations in order to examine effects of different theoretical approximations.

## 3. Results and discussions

A set of complete total energy calculations for (1 1 0), and (0 0 1), (1 1 1) surfaces at all six theoretical levels indicate that lowest total energy is obtained at the AFM-SO level, indicating the ground state is AFM-SO. Thus, the present study is dedicated to comparatively study the quantum size effects (QSE) in the (1 1 0), (0 0 1) and (1 1 1) fcc Am surfaces at the ground state of AFM-SO. It is commonly believed that surface energy and work function are two parameters, which are sensitive to QSE [28,29]. We have calculated the work function,  $W$ , according to the following formula :

$$W = V_0 - E_F, \quad (1)$$

where  $V_0$  is the Coulomb potential energy at the half height of the slab including the vacuum layer and  $E_F$  is the Fermi energy. The work functions of fcc Am (1 1 0), (0 0 1) and (1 1 1) films up to seven layers have been calculated at the AFM-SO level, and the results are listed in Table 1 and plotted in Fig. 1 as well. Several

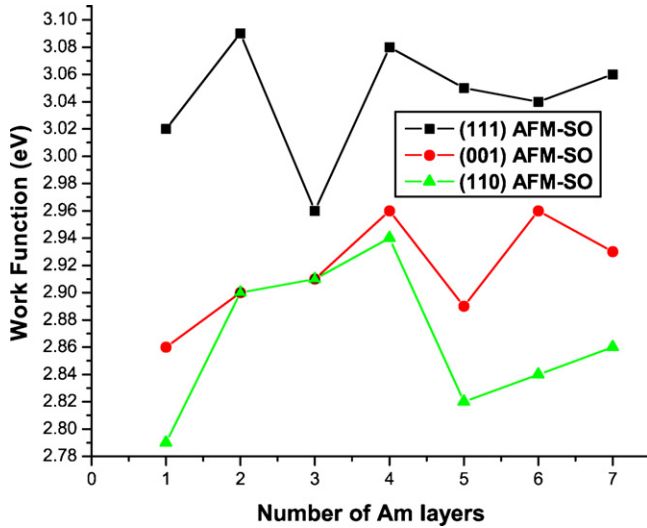


Fig. 1. Work functions of fcc Am (1 1 0), (0 0 1) and (1 1 1) films as a function of the number of layers up to seven layers ( $N=1-7$ ) at the AFM-SO level.

features can be observed from these results: (1) a strong QSE is observed for both fcc Am (1 1 0) and (0 0 1) films up to seven layers while the work function for fcc Am (1 1 1) films becomes relatively stable as the number of layers reaches five. This indicates that for fcc Am (1 1 0) and (0 0 1) surfaces, film thickness greater than seven is required for any chemisorption study that requires an accurate prediction of the adsorbate-induced work function shift. On the other hand, a five-layer fcc Am (1 1 1) film may be sufficient for any future adsorption investigation that requires an accurate prediction of the adsorbate-induced work function shift. Compared with  $\delta$ -Pu [27], our results indicate that QSE is more pronounced in Am surfaces than in corresponding  $\delta$ -Pu surfaces, especially in the (0 0 1) surface. (2) The work functions of fcc Am surfaces have a decreasing sequence as (1 1 1)  $\rightarrow$  (0 0 1)  $\rightarrow$  (1 1 0). A similar trend has been observed for the  $\delta$ -Pu surfaces [27]. The sequence of work functions is reasonable and it is consistent with the stability of these three surfaces, *i.e.*, (1 1 1) surface is the most stable surface and the energy needed to move the electron far from the surface is therefore the highest, and in turn the (0 0 1) and (1 1 0) surfaces. (3) At the ground state, the work functions for fcc Am (1 1 0), (0 0 1), and (1 1 1) films with seven layers are calculated to be 2.86, 2.93, and 3.06 eV, respectively. We note that these values are smaller than the corresponding work function values, namely 2.99, 3.11, and 3.41 eV, of  $\delta$ -Pu surfaces at the same level of theory [27].

The surface energy for a  $N$ -layer film has been estimated from [43]:

$$E_s = \frac{1}{2}[E_{\text{tot}}(N) - NE_B], \quad (2)$$

where  $E_{\text{tot}}(N)$  is the total energy of the  $N$ -layer slab and  $E_B$  is the energy of the infinite crystal. If  $N$  is sufficiently large and  $E_{\text{tot}}(N)$  and  $E_B$  are known to infinite precision, Eq. (2) is exact. If, however, the bulk and film calculations are not entirely consistent with each other,  $E_s$  will diverge linearly with increasing  $N$ . Stable and internally consistent estimates of  $E_s$  and  $E_B$  can, however, be extracted from a series of values of  $E_{\text{tot}}(N)$  via a

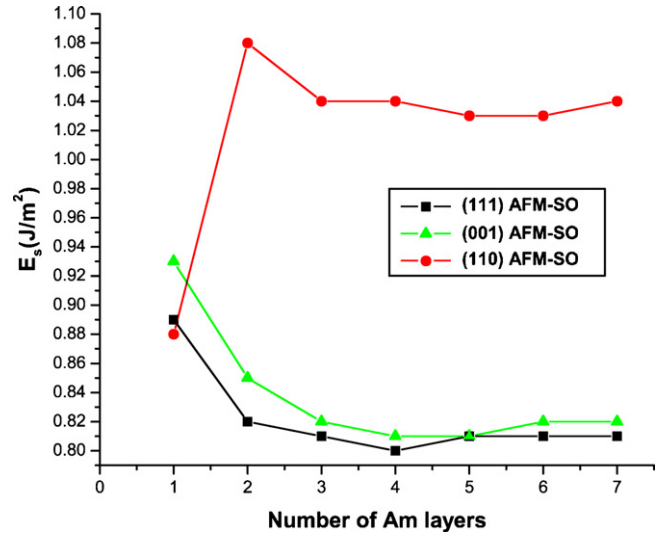


Fig. 2. Surface energies of fcc Am (1 1 0), (0 0 1), and (1 1 1) films as a function of the number of layers with  $N=1-7$  at the AFM-SO level.

linear least-squares fit to [44]:

$$E_{\text{tot}}(N) = E_B N + 2E_s. \quad (3)$$

To obtain an optimal result, the fit to Eq. (3) should only be applied to films which include, at least, one bulk-like layer, *i.e.*,  $N > 2$ . We have independently applied this fitting procedure to the fcc Am (1 1 0) films at the ground state, respectively. The surface energy for each film has been computed using the calculated  $N$ -layer total energy and appropriately fitted bulk energy. The results are listed in Table 1 and plotted in Fig. 2 and compared with the results for (0 0 1) and (1 1 1) surfaces. Several features of the surface energies are evident from our results. First, for all three surfaces, the surface energy converges pretty well to the corresponding semi-infinite surface energy when the number of layers reaches three, which agrees well with the surface energy behavior of  $\delta$ -Pu (1 1 0), (1 1 1) and (0 0 1) films up to seven layers [27]. From these observations, we again infer, similar to the (1 1 0), (0 0 1) and (1 1 1) surfaces of  $\delta$ -Pu [27], that a three layer film may be sufficient for future atomic and molecular adsorption studies on fcc Am films, if the primary quantity of interest is the chemisorption energy. Second, the (1 1 0) surface has the highest surface energy and (1 1 1) surface the lowest, while (0 0 1) surface is intermediate between the (1 1 0) surface and (1 1 1) surface. Similar to the observed work function sequence, the sequence of surface energy is consistent with the stability of these three surfaces, *i.e.*, fcc Am (1 1 0) surface is the most unstable and (1 1 1) is the most stable, while the stability of the (0 0 1) surface is intermediate between those of the (1 1 0) and (1 1 1) surfaces. Third, though the film thickness dependence and sequence of surface energies in fcc Am are similar to those in  $\delta$ -Pu [27], the surface energies of fcc Am is much smaller than the corresponding  $\delta$ -Pu surface energies. At the ground state, the surface energies of (1 1 0), (0 0 1) and (1 1 1) fcc Am films are predicted to be 1.04, 0.82, and 0.81 J/m<sup>2</sup>, respectively, while the corresponding value for  $\delta$ -Pu films are 1.42, 1.21, and 1.18 J/m<sup>2</sup>.

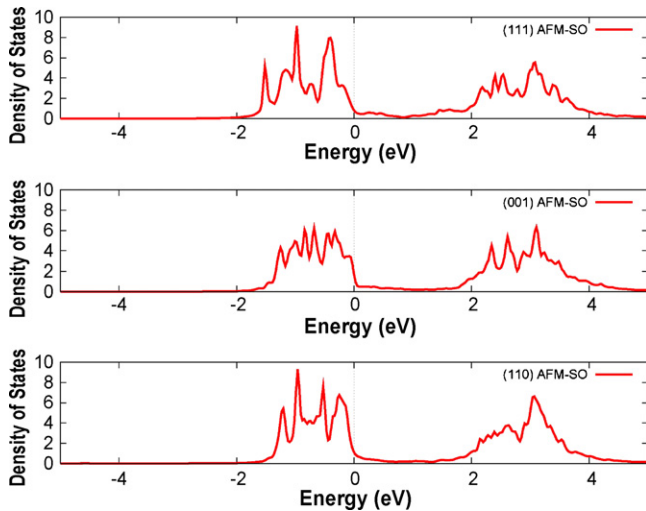


Fig. 3. Density of states for 5f electrons in fcc Am (110), (001), and (111) films with seven layers at the AFM-SO level.

The density of states (DOS) for 5f electrons of fcc Am (110), (001), and (111) films are presented at the AFM-SO level with seven layers in Fig. 3. From the figure, we first note that in all three surfaces the two 5f peaks, one below the Fermi level while the other above the Fermi level, are well separated by a wide gap indicating that the 5f electrons are localized. The gap width is about 2 eV for all three surface calculations, which is in a good agreement with the gap width found in the bulk dhcp Am [5] and bulk fcc Am [23]. In addition, compared to (110) and (001) surface, the center of the first peak in (111) surface appears to be moving further away from the Fermi level. In contrast to this, there is only one broad peak across the Fermi level in all three  $\delta$ -Pu films [27], indicating that the 5f electrons in  $\delta$ -Pu surfaces are more delocalized than the 5f electrons in fcc Am surfaces.

We now specifically comment on some electronic structure properties of fcc Am (110) surface. The spin magnetic moment per atom of fcc Am (110) films up to seven layers has been calculated at the SP-NSO, SP-SO, AFM-NSO, and AFM-SO levels, respectively, and the results are listed in Table 2. From the table, several features have been observed for the magnetic properties. First, for the Am (110) films at both AFM-NSO and AFM-SO levels, the magnetic moment becomes smaller with the increase of the number of layers, and it is expected that the magnetic moment will finally approach zero. A similar trend has been observed in our previous  $\delta$ -Pu surface studies [27]. Second, for the Am (110) films at the SP-NSO and SP-SO levels, the magnetic moments are, in general, larger than the corresponding bulk values of 7.32 and 6.90  $\mu_B$ /atom [19], and with the increase of the number of layers the magnetic moments quickly approach the values of the corresponding bulks. For the seven layers thick film, the magnetic moment at the SP-NSO and SP-SO levels is 7.37 and 6.98  $\mu_B$ /atom already. The spin magnetic moments of  $\delta$ -Pu (110) films at the SP-NSO and SP-SO levels show a similar feature as found here except that the magnetic moments of  $\delta$ -Pu (110) films are smaller than the corresponding magnetic moments of Am (110) films. The difference is attributed to the additional 5f electron in Am.

Table 2

Magnetic moments MM per atom ( $\mu_B$ /atom), spin polarization energies per atom  $E_{SP}$ , spin orbit coupling energies per atom  $E_{SO}$ , for the fcc Am (110)  $N$  layers ( $N = 1-7$ )

$N$	Theory	MM ( $\mu_B$ /atom)	$E_{SP}$ (eV/atom)	$E_{SO}$ (eV/atom)
1	NSP-SO			9.52
	SP-NSO	7.63	4.47	
	SP-SO	7.43	2.46	7.51
	AFM-NSO	7.74	4.54	
	AFM-SO	7.42	2.55	7.53
2	NSP-SO			8.77
	SP-NSO	7.79	2.92	
	SP-SO	7.49	1.75	7.61
	AFM-NSO	0	2.84	
	AFM-SO	0	1.69	7.62
3	NSP-SO			8.75
	SP-NSO	7.53	2.72	
	SP-SO	7.19	1.63	7.65
	AFM-NSO	2.44	2.69	
	AFM-SO	2.38	1.60	7.66
4	NSP-SO			8.74
	SP-NSO	7.42	2.65	
	SP-SO	7.05	1.58	7.66
	AFM-NSO	0	2.62	
	AFM-SO	0	1.57	7.69
5	NSP-SO			8.75
	SP-NSO	7.51	2.63	
	SP-SO	7.12	1.56	7.67
	AFM-NSO	1.44	2.60	
	AFM-SO	1.37	1.57	7.71
6	NSP-SO			8.75
	SP-NSO	7.39	2.61	
	SP-SO	7.00	1.54	7.68
	AFM-NSO	0	2.59	
	AFM-SO	0	1.56	7.72
7	NSP-SO			8.74
	SP-NSO	7.37	2.59	
	SP-SO	6.98	1.53	7.69
	AFM-NSO	1.03	2.58	
	AFM-SO	0.99	1.56	7.72

The cohesive energy for the fcc Am (110)  $N$ -layer films with respect to  $N$  monolayers is calculated and plotted in Fig. 4. It is found that the cohesive energy increases monotonously with the film thickness at all six levels of calculations. It is also observed that the rate of increase of cohesive energy drops significantly as the number of layers increases, which has been previously noticed for the cohesive energy of  $\delta$ -Pu (110) surface as well, and we expect that the convergence in the cohesive energy can be achieved after a few more layers. However, since to the best of our knowledge, the experimental value for the semi-infinite surface cohesive energy is not known, we are unable to predict how many layers will be needed to achieve the semi-infinite surface energy. From the figure, obviously, spin polarization significantly lowers the cohesive energy at both the scalar relativistic and fully relativistic levels of theory. On the other hand, spin-orbit coupling increases the cohesive energy of the spin-polarized  $N$ -layers by about  $\sim 11$ – $13\%$  but reduces the cohesive energy of the non-spin-polarized  $N$ -layers by about  $\sim 23$ – $27\%$ .

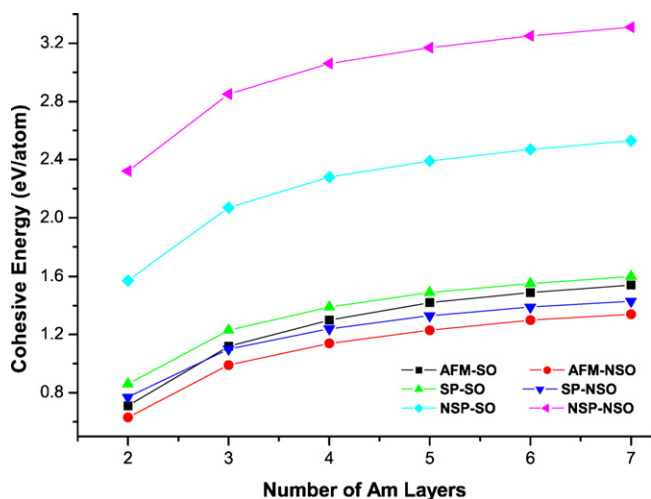


Fig. 4. Cohesive energy per atom of the fcc Am (1 1 0) films with respect to the Am monolayer vs. the number of Am layers.

These features are in general agreement with the results of  $\delta$ -Pu (1 1 0) surface [27]. At the antiferromagnetic state, spin-orbit coupling increases the cohesive energy of the  $N$ -layers by about  $\sim 12$ – $15\%$ . All cohesive energies are positive, indicating that all layers of Am (1 1 0) films are bound relative to the monolayer.

To further understand the effects brought by the spin polarization and the spin-orbit coupling, we also calculated spin-polarization energies and spin-orbit coupling energies for the fcc Am (1 1 0) films at various theoretical levels, and the results are shown in Table 2 as well as in Figs. 5 and 6. The spin-polarization energy  $E_{SP}$  is defined by:

$$E_{SP} = E_{\text{tot}}(\text{NSP}) - E_{\text{tot}}(\text{SP}), \quad (4)$$

and the spin-orbit coupling energy  $E_{SO}$  is defined by:

$$E_{SO} = E_{\text{tot}}(\text{NSO}) - E_{\text{tot}}(\text{SO}). \quad (5)$$

Our results showed that both spin polarization energies and spin orbit coupling energies become pretty stable when the number

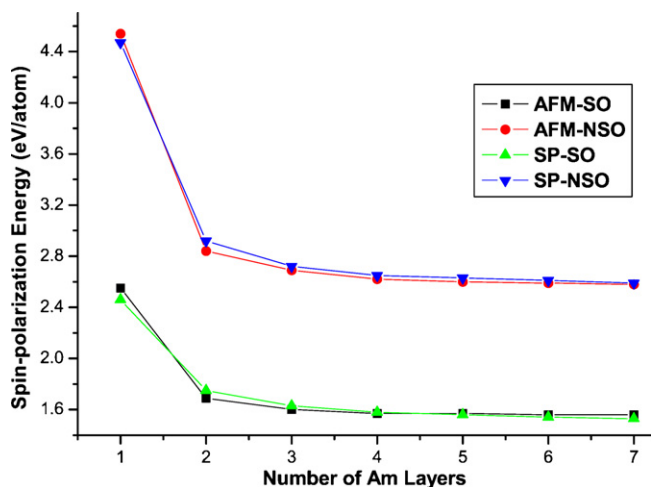


Fig. 5. Spin-polarization energy (eV/atom) of a  $N$ -layer fcc Am (1 1 0) films as a function of the number of Am layers with  $N=1$ – $7$ .

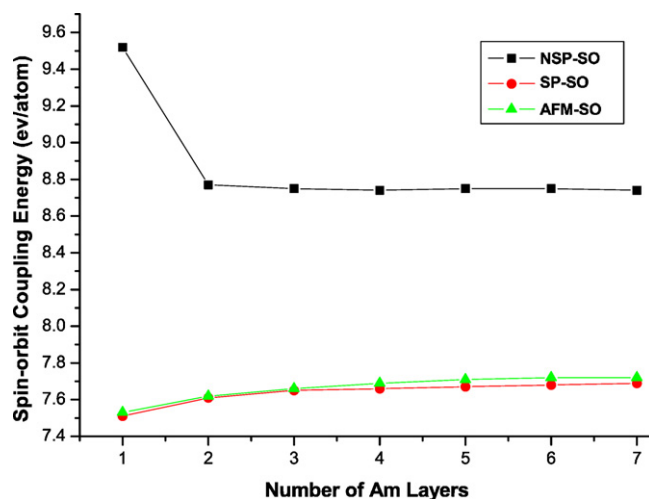


Fig. 6. Spin-orbit coupling energy (eV/atom) of a  $N$ -layer fcc Am (1 1 0) films as a function of the number of Am layers with  $N=1$ – $7$ .

of layers reaches three. Moreover, the spin-orbit coupling plays a more important role than the spin-polarization in reducing the total energies of the fcc Am (1 1 0) films, *i.e.*, the spin-orbit coupling effect reduces the total energy by 7.51–9.52 eV/atom, while spin-polarization effect decreases the total energy only by 1.53–4.54 eV/atom. Comparing these to the SO coupling and SP effects in the  $\delta$ -Pu (1 1 0) films, which are 5.97–8.56 eV/atom and 0.46–3.08 eV/atom, respectively [27], the effects in fcc Am (1 1 0) films are more pronounced. Such discrepancy can also be partially attributed to the additional 5f electron in Am and the localized feature of these electrons.

In summary, we have reported a comparative study of the three high symmetry surfaces of fcc Am(II). Our present work provides the first comparative electronic structure results for all three fcc Am high symmetry surfaces as well as a detailed comparison with the corresponding  $\delta$ -Pu surfaces. It is found that the 5f electrons in the three fcc Am surfaces are primarily localized, of which the (1 1 1) surface is probably most localized. It is also observed that the surface energies have an increasing sequence as (1 1 1)  $\rightarrow$  (0 0 1)  $\rightarrow$  (1 1 0), while the work function shows a strong quantum size effect for fcc Am (1 1 0) and (0 0 1) films up to seven layers and for fcc Am (1 1 1) up to five layers. Moreover, for the fcc Am (1 1 0) surfaces, it is predicted that the spin-orbit coupling plays a more important role than the spin-polarization in reducing the total energies of the fcc Am (1 1 0) films. We also note that the spin polarization may significantly lower the cohesive energy at both the scalar relativistic and fully relativistic levels of theory.

## Acknowledgements

This work is supported by the Chemical Sciences, Geosciences and Biosciences Division, Office of Basic Energy Sciences, Office of Science, U.S. Department of Energy (Grant no. DE-FG02-03ER15409) and the Welch Foundation, Houston, Texas (Grant no. Y-1525).

## References

- [1] J.J. Katz, G.T. Seaborg, L.R. Morss, *The Chemistry of the Actinide Elements*, Chapman and Hall, 1986;  
L.R. Morss, J. Fuger (Eds.), *Transuranium Elements: A Half Century*, American Chemical Society, Washington, DC, 1992;  
L.R. Morss, *Mater. Res. Soc. Symp. Proc.* 802 (2004) (DD 4.1.1).
- [2] J.J. Katz, L.R. Morss, J. Fuger, N.M. Edelstein (Eds.), *Chemistry of the Actinide and Transactinide Elements*, Springer, New York, 2006.
- [3] R. Haire, S. Heathman, M. Idiri, T. Le Bihan, A. Lindbaum, *Nuclear Materials Technology*, Los Alamos National Laboratory, 2003, 3rd/4th quarter, p. 23.
- [4] Proceedings of the Robert A. Welch Foundation, Houston, Texas, October 22–23, 1990.
- [5] Actinides 2005, Proceedings of the Materials Research Society Symposium, vol. 893, 2006.
- [6] G.T. Seaborg, W.D. Loveland, *The Elements Beyond Uranium*, John Wiley & Sons Inc., 1990, p. 17.
- [7] S. Heathman, R.G. Haire, T. Le Bihan, A. Lindbaum, K. Litfin, Y. Méresse, H. Libotte, *Phys. Rev. Lett.* 85 (2000) 2961.
- [8] G.H. Lander, J. Fuger, *Endeavour* 13 (8) (1989).
- [9] A.J. Freeman, D.D. Koelling, in: A.J. Freeman, J.B. Darby Jr. (Eds.), *The Actinides: Electronic Structure and Related Properties*, Academic, New York, 1974.
- [10] B. Johansson, *Phys. Rev. B* 11 (1975) 2740.
- [11] H.L. Skriver, O.K. Andersen, B. Johansson, *Phys. Rev. Lett.* 41 (1978) 42.
- [12] J.R. Naegele, L. Manes, J.C. Spirlet, W. Müller, *Phys. Rev. Lett.* 52 (1984) 1834.
- [13] A. Lindbaum, S. Heathman, K. Litfin, Y. Méresse, *Phys. Rev. B* 63 (2001) 214101.
- [14] M. Pénicaud, *J. Phys. Condens. Matter* 17 (2005) 257.
- [15] S.Y. Savrasov, K. Haule, G. Kotliar, *Phys. Rev. Lett.* 96 (2006) 036404.
- [16] P. Söderlind, A. Landa, *Phys. Rev. B* 72 (2005) 024109.
- [17] P.G. Huray, S.E. Nave, R.G. Haire, *J. Less-Com. Met.* 93 (1983) 293.
- [18] T. Gouder, P.M. Oppeneer, F. Huber, F. Wastin, J. Rebizant, *Phys. Rev. B* 72 (2005) 115122;  
L.E. Cox, J.W. Ward, R.G. Haire, *Phys. Rev. B* 45 (1992) 13239.
- [19] D. Gao, A.K. Ray, *Eur. Phys. J. B* 50 (2006) 497;  
D. Gao, A.K. Ray, Proceedings of the MRS Fall 2005 Symposium, vol. 893, 2006, p. 39;  
D. Gao, A.K. Ray, *Surf. Sci.*, in press.
- [20] O. Eriksson, J.M. Wills, *Phys. Rev. B* 45 (1992) 3198.
- [21] A.L. Kutepov, S.G. Kutepova, *J. Magn. Magn. Mater.* 272–276 (2004) e329.
- [22] A. Shick, L. Havela, J. Kolorenc, V. Drchal, T. Gouder, P.M. Oppeneer, *Phys. Rev. B* 73 (2006) 104415.
- [23] S.Y. Savrasov, G. Kotliar, E. Abrahams, *Nature* 410 (2001) 793;  
G. Kotliar, D. Vollhardt, *Phys. Today* 57 (2004) 53;  
X. Dai, S.Y. Savrasov, G. Kotliar, A. Migliori, H. Ledbetter, E. Abrahams, *Science* 300 (2003) 953;  
B. Johansson, *Phys. Rev. B* 11 (1975) 2740.
- [24] B. Johansson, A. Rosengren, *Phys. Rev. B* 11 (1975) 2836.
- [25] J.L. Smith, R.G. Haire, *Science* 200 (1978) 535.
- [26] J.C. Griveau, J. Rebizant, G.H. Lander, G. Kotliar, *Phys. Rev. Lett.* 94 (2005) 097002.
- [27] X. Wu, A.K. Ray, *Phys. Rev. B* 72 (2005) 045115;  
A.K. Ray, J.C. Boettger, *Phys. Rev. B* 70 (2004) 085418;  
J.C. Boettger, A.K. Ray, *Int. J. Quant. Chem.* 105 (2005) 564;  
M.N. Huda, A.K. Ray, *Eur. Phys. J. B* 40 (2004) 337;  
M.N. Huda, A.K. Ray, *Physica B* 352 (2004) 5;  
M.N. Huda, A.K. Ray, *Eur. Phys. J. B* 43 (2005) 131;  
M.N. Huda, A.K. Ray, *Physica B* 366 (2005) 95;  
M.N. Huda, A.K. Ray, *Phys. Rev. B* 72 (2005) 085101;  
M.N. Huda, A.K. Ray, *Int. J. Quant. Chem.* 105 (2005) 280;  
H.R. Gong, A.K. Ray, *Eur. Phys. J. B* 48 (2005) 409;  
H.R. Gong, A.K. Ray, Proceedings of the MRS Fall 2005 Symposium, vol. 893, 2006, p. 45;  
H.R. Gong, A.K. Ray, *Surf. Sci.* 600 (2006) 2231.
- [28] E.K. Schulte, *Surf. Sci.* 55 (1976) 427.
- [29] P.J. Feibelman, *Phys. Rev. B* 27 (1982) 1991.
- [30] E.E. Mola, J.L. Vicente, *J. Chem. Phys.* 84 (1986) 2876.
- [31] I.P. Bartra, S. Ciraci, G.P. Srivastava, J.S. Nelson, C.Y. Fong, *Phys. Rev. B* 34 (1986) 8246.
- [32] J.C. Boettger, S.B. Trickey, *Phys. Rev. B* 45 (1992) 1363;  
J.C. Boettger, *Phys. Rev. B* 53 (1996) 13133.
- [33] C.M. Wei, M.Y. Chou, *Phys. Rev. B* 66 (2002) 233408.
- [34] E. Stjöstedt, L. Nordström, D.J. Singh, *Solid State Commun.* 114 (2000) 15.
- [35] P. Blaha, K. Schwarz, P.I. Sorantin, S.B. Trickey, *Comp. Phys. Commun.* 59 (1990) 399;  
M. Petersen, F. Wagner, L. Hufnagel, M. Scheffler, P. Blaha, K. Schwarz, *Comp. Phys. Commun.* 126 (2000) 294;  
K. Schwarz, P. Blaha, G.K.H. Madsen, *Comp. Phys. Commun.* 147 (2002) 71.
- [36] P. Hohenberg, W. Kohn, *Phys. Rev.* 136 (1964) B864;  
W. Kohn, L.J. Sham, *Phys. Rev.* 140 (1965) A1133;  
S.B. Trickey (Ed.), *Density Functional Theory for Many Fermion Systems*, Academic, San Diego, 1990;  
R.M. Dreier, E.K.U. Gross, *Density Functional Theory: An Approach to Quantum Many Body Problem*, Springer, Berlin, 1990;  
J.F. Dobson, G. Vignale, M.P. Das (Eds.), *Electronic Density Functional Theory Recent Progress and New Directions*, Plenum, New York, 1998.
- [37] J.P. Perdew, K. Burke, M. Ernzerhof, *Phys. Rev. Lett.* 77 (1996) 3865;  
J.P. Perdew, K. Burke, Y. Wang, *Phys. Rev. B* 54 (1996) 16533;  
J.P. Perdew, in: Ziesche, H. Eschrig (Eds.), *Electronic Structure of Solids*, Akademie Verlag, Berlin, 1991.
- [38] P.E. Blöchl, O. Jepsen, O.K. Andersen, *Phys. Rev. B* 49 (1994) 16223.
- [39] G.K.H. Madsen, P. Blaha, K. Schwarz, E. Sjustedt, L. Nordstrom, *Phys. Rev. B* 64 (2001) 195134.
- [40] D.D. Koelling, B.N. Harmon, *J. Phys. C: Solid State Phys.* 10 (1977) 3107.
- [41] A.H. MacDonald, W.E. Pickett, D.D. Koelling, *J. Phys. C: Solid State Phys.* 13 (1980) 2675.
- [42] P. Novak, \$WIENROOT/SRC/novak.lecture\_on.spinorbit.ps(WIEN97).
- [43] J.G. Gay, J.R. Smith, R. Richter, F.J. Arlinghaus, R.H. Wagoner, *J. Vac. Sci. Technol. A* 2 (1984) 931.
- [44] J.C. Boettger, *Phys. Rev. B* 49 (1994) 16798.